

## EXPERIMENT AND PARAMETER OPTIMIZATION OF ROOT-CUTTING FOR TRIMMING POSTHARVEST CABBAGE

### 甘蓝采后整修切根试验与参数优化

Cui Gongpei <sup>1,2)</sup>, Wei Yongzhe, <sup>1,2)</sup>; Wen Shuangtao <sup>1,3)</sup>, Zheng Xinmeng <sup>1)</sup>, Wang Jingzheng <sup>1)</sup>, Cui Yongjie <sup>\*1,3)</sup> <sup>1</sup>

<sup>1)</sup> College of Mechanical and Electronic Engineering, Northwest A&F University, Yangling / China;

<sup>2)</sup> Key Laboratory of Agricultural Internet of Things, Ministry of Agriculture and Rural Affairs, Yangling / China;

<sup>3)</sup> Shaanxi Key Laboratory of Agricultural Information Perception and Intelligent Service, Yangling / China

Tel: +86 13720581232; E-mail: agriculturalrobot@nwfau.edu.cn

DOI: <https://doi.org/10.35633/inmateh-63-41>

**Keywords:** postharvest cabbage, trimming, root-cutting, morphology, parameter optimization

#### ABSTRACT

Trimming for postharvest cabbage is useful to increase its economic value added. For obtaining the optimal root-cutting parameters, a root-cutting test platform based on universal testing machine was designed. Then shear contrast test and orthogonal test were carried out respectively, and shear properties were explained according to root morphology obtained by scanning electron microscope (SEM). The results showed that the effect of sliding-cutting with single-edged cutter was the best. The optimal parameters of cutter thickness, shear position, shear speed and sliding-cutting angle were respectively 0.89 mm, 0.00 mm, 388.94 mm/min and 34.84°, and the shear stress was 28.02 kPa.

#### 摘要

采后甘蓝整修有利于提升其经济附加值。为了获得采后甘蓝较佳的切根参数，本文基于万能试验机设计了一种切根试验平台。分别进行了剪切对比试验和正交试验，并根据扫描电子显微镜获取的根部形貌对剪切特性进行了分析。结果表明：单平刃滑切作业效果最佳；最优参数组合为刀具厚度 0.89 mm，剪切位置 0.00 mm，剪切速度 388.94 mm/min，滑切角 34.84°，剪切应力为 28.02 kPa。

#### INTRODUCTION

Efficiency and performance of existing cabbage harvesters have basically met the requirements of husbandmen (Toncheva et al., 2017; Zhou et al., 2017; Du et al., 2019). But the root of harvested cabbage is too long, which seriously affects the appearance of cabbage products and easily causes economic losses (Du, 2017). Thus root-cutting and other operations of postharvest trimming are needed to enhance the economic value added of cabbage products (Cui et al., 2019).

At present, the reported studies on the root-cutting of cabbage mainly focus on the harvesting in the field. Li, X. Q. et al. determined the optimal cutting position was 5~40 mm from the top leaf (Li et al., 2013). Du, D. D. et al. determined that the preferred cutting area was 30~35 mm in root diameter, and the test results were analysed by combining the average moisture content and crude fibre content (Du, Wang and Qiu, 2014). Subsequently, the splitting of root-cutting was analysed through a mechanical model (Du, Wang and Qiu, 2015). Li, T. H. et al. designed an adjustable device for root cutting, and a mathematical model between the maximum root cutting reaction force and various factors was established to obtain the optimal parameter combination (Li et al., 2020).

Above researches of the root-cutting near top leaf during harvesting cannot be applied to trimming closer to the cabbage head during postharvest treatment. Therefore, this paper designs a root-cutting test platform based on the universal testing machine, according to the achievement of our research team on the automatic orientation of postharvest cabbage (Zheng et al., 2021). Then shear contrast test and orthogonal test are carried out, and the optimal shear form and operating parameter combination are obtained, which provides a theoretical basis for designing and improving the root-cutting device of the postharvest cabbage automatic trimming equipment.

<sup>1</sup> Gongpei Cui, Ph.D. Stud. Eng.; Yongzhe Wei, M.S. Stud. Eng.; Shuangtao Wen, M.S. Stud. Eng.; Xinmeng Zheng, M.S. Stud. Eng.; Jingzheng Wang, M.S. Stud. Eng.; Yongjie Cui, Prof. Ph.D. Eng.

## MATERIALS AND METHODS

### Samples

Fresh "Zhonggan No.15" cabbages cultivated at Taibai Vegetable Experiment and Demonstration Station of Northwest A&F University (Shaanxi Province, China) were used for the root-cutting experiment in this study. Outer leaves and roots of all cabbage samples were preserved during harvesting in order to maintain the mechanical properties. A total of 172 cabbage samples were collected in July 2019, and these cabbages were checked again to ensure that they were not infested or infected after being properly transported to the laboratory. Then, the outer leaves of cabbage were removed manually and the surface was cleaned. The physical parameters of postharvest cabbage are reported in Table 1. All samples were stored in a refrigerator with a temperature of about 3°C, and the relevant tests were completed within 72 hours at room temperature ( $24 \pm 1^\circ\text{C}$ , 50–55% Rh).

Table 1

Physical parameters of postharvest cabbage

	Cross diameter	Longitudinal diameter	Height	Root diameter
	[mm]	[mm]	[mm]	[mm]
Maximum	143.48	138.75	170.49	34.05
Minimum	106.37	96.99	126.01	28.26
Mean	129.27	119.10	149.02	31.43
Standard deviation	9.45	9.40	11.39	1.72

### Root-cutting test platform

To further study the shear properties of root, a root-cutting test platform for cabbage based on the universal testing machine (HY-0230, Hengyi, Shanghai) was designed, consisting of adjusting mechanism for cutter, cutter, gripper, support, etc. The structure is shown in Fig. 1.

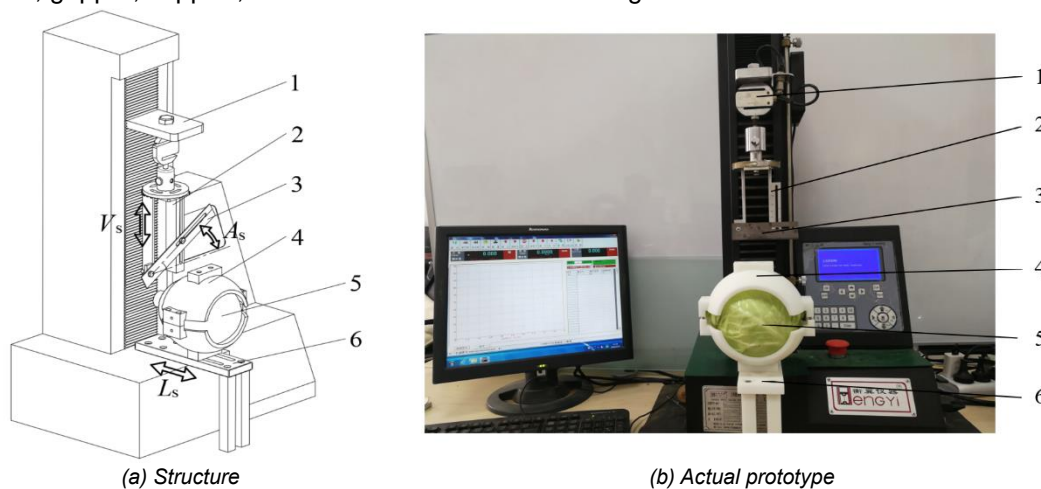


Fig. 1 - Root-cutting test platform for cabbage

1 - universal testing machine; 2 - adjusting mechanism for cutter; 3 - cutter; 4 - gripper; 5 - cabbage; 6 - support;  $V_s$  - shear speed, mm/min;  $A_s$  - sliding-cutting angle, °;  $L_s$  - shear position, mm.

Specifically, the postharvest cabbage was fixed by two 3D-printed profile modeling grippers, and the root was exposed to outside the gripper. The gripper was connected to the support fixed on the universal testing machine, and the shear position ( $L_s$ ) can be changed by adjusting the positional relationship between the gripper and support. At the same time, the adjusting mechanism for cutter was connected to the chuck of force sensor on the universal testing machine, and the shear speed ( $V_s$ ) was controlled by changing the parameter of loading speed. The cutter and the root of cabbage formed an angle of  $90^\circ$  to ensure the flatness of root-cutting surface (USDA, 1997). One side of the cutter was hinged with the adjusting mechanism for cutter, and the other side was connected with a sliding pair to adjust the sliding-cutting angle ( $A_s$ ). The root diameter has been measured to be  $31.43 \pm 1.72$  mm (shown in Table 1), thus the horizontal spacing of the adjusting mechanism for cutter was determined to be 55 mm to ensure the successful root-cutting.

In this study, shear stress was used as the test index to avoid the influence of individual differences on results (Ghahraei et al., 2011; Ma et al., 2019), which can be calculated by equation (1) and equation (2).

Here, the value of the highest point of root-cutting curve was selected as the maximum root-cutting force ( $F_{max}$ ), and the area of shear cross-section ( $S$ ) was calculated from the diameter of shear cross-section ( $D_T$ ).

$$\begin{cases} P_s = \frac{F_{max}}{S} \\ S = \frac{\pi D_T^2}{4} \end{cases} \quad (1)$$

$$P_s = \frac{4F_{max}}{\pi D_T^2} \quad (2)$$

where:  $P_s$  is the shear stress, [Pa];  $F_{max}$  is the maximum root-cutting force, [N];  $S$  is the area of shear cross-section, [m<sup>2</sup>];  $D_T$  is the diameter of the shear cross-section, [m].

The specific steps of the root-cutting test are as follows: When the cutter approached the root with a constant loading speed, the signal of force sensor was reset. Then the cutter displacement and root-cutting force were measured by displacement sensor and force sensor respectively, and the root-cutting curve was obtained. The test was repeated three times for each group, and the mean value was taken as the test result. Among them, 72 cabbages were used for shear contrast test, 90 cabbages were used for shear orthogonal test, and 10 cabbages were used for verification test.

### Shear contrast test

In order to obtain optimal shear form, the shear contrast test was carried out, and it provided a theoretical basis for subsequent shear orthogonal test. The specific test factors are described in Table 2. The thickness of cutter was 1mm, and the angle of sliding-cutting was selected as 40° (Du, Wang and Qiu, 2015). The shear position refers to the distance from the cutter to the joint of the root and the head, and the longest length of root met trimming requirement was 20 mm (MOA, 2002). In addition, the loading speed of the universal testing machine was consistent in each group of tests, all of which were 300 mm/min.

**Table 2**

Factors of shear contrast test		
Cutter type	Sliding-cutting angle	Shear position
	[°]	[mm]
Single-edged cutter	0 (Flat cutting)	20
		16
		12
Double-edged cutter	40 (Sliding cutting)	8
		4
		0

### Shear orthogonal test

In order to obtain the optimal parameter combination for root-cutting of postharvest cabbage, a shear orthogonal test was conducted. The cutter thickness ( $T_c$ ), shear position ( $L_s$ ), shear speed ( $V_s$ ) and sliding-cutting angle ( $A_s$ ) were used as the test factors, and the shear stress ( $P_s$ ) was used as the test index. According to the results of the shear contrast test, the cutter type of this test was selected as a single-edged cutter, and the range of shear position was from 0 mm to 12 mm. At the same time, the ranges of other test factors were determined by trial tests. The factor codes of the shear orthogonal test are shown in Table 3.

**Table 3**

Factor codes of shear orthogonal test				
Code	Cutter thickness	Shear position	Shear speed	Sliding-cutting angle
	[mm]	[mm]	[mm/min]	[°]
2(r)	1.4	12	500	50
1	1.2	9	400	40
0	1.0	6	300	30
-1	0.8	3	200	20
-2(-r)	0.6	0	100	10

### Morphology analysis of root by SEM

In order to explain the root-cutting properties better, the microscopic morphology of the root tissue was achieved by SEM (Nano SEM-450, FEI, USA). Firstly, the samples of cambium and xylem were taken from the shear cross-section of root, and prepared into 6×6 mm slices with a thickness of 1 mm. Subsequently, the critical-point drying method (Xu and Yang, 2008) was used to fix, rinse, dehydrate, do critical-point drying and gold spraying, etc. Finally, the samples were observed under the SEM with 200 times magnification.

## RESULTS

### Analysis of shear properties by root morphology

The typical curve of root-cutting force with cutter displacement is shown in Fig. 2(a). Which was bimodal and could be divided into three stages ( $D_1$ ,  $D_2$  and  $D_3$ ). Specifically, the root-cutting force at stage  $D_1$  increased linearly with cutter displacement until it reached the first peak  $P_1$ . In the stage  $D_2$ , the root-cutting force fell from the peak value and remained stable within certain displacement range, and then increased linearly to the second peak  $P_2$ . Finally, the root-cutting force at stage  $D_3$  decreased approximately linearly with cutter displacement until the end of root-cutting.

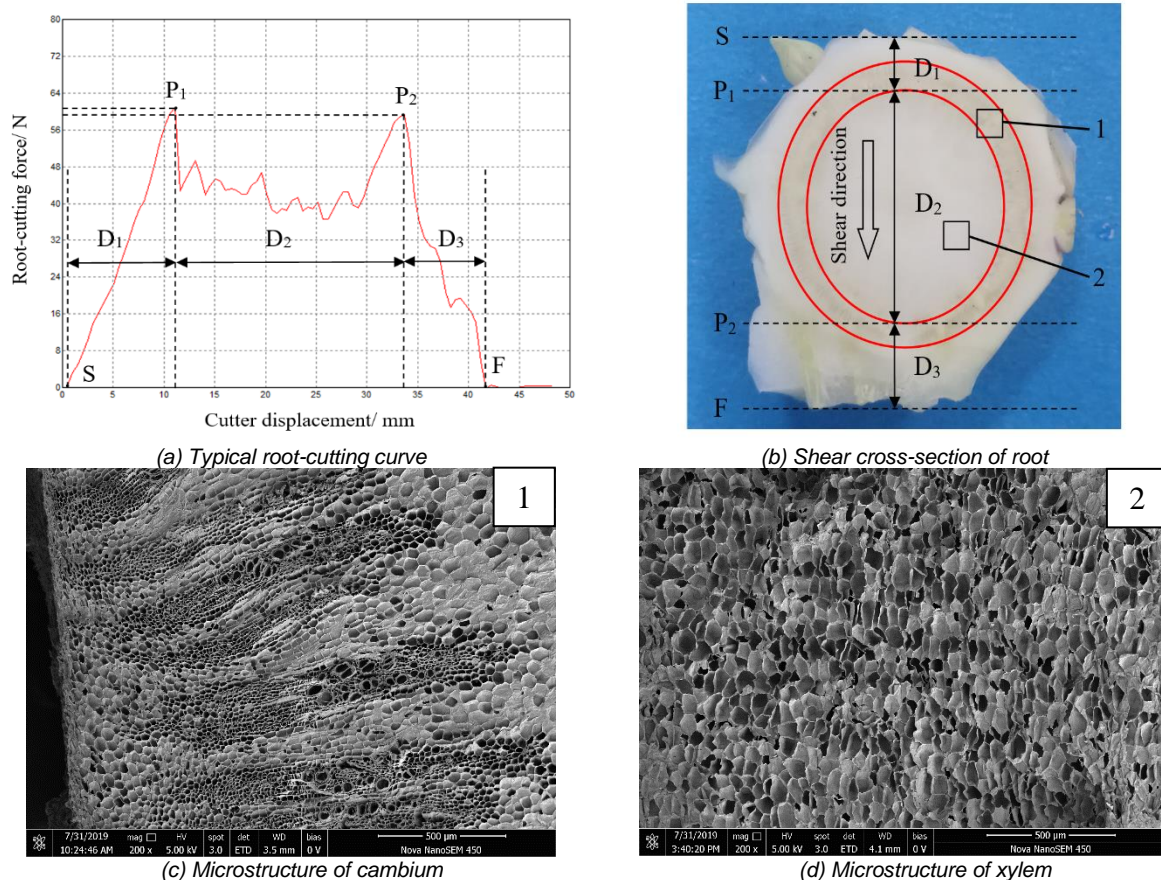


**Fig. 2 - Analysis of shear properties**

$S$  - start of root-cutting;  $P_1$ ,  $P_2$  - peaks of root-cutting;  $F$  - end of root-cutting;  $D_1$ ,  $D_2$ ,  $D_3$  - different stages of root-cutting; 1 - cambium; 2 - xylem.

The shear properties were explained according to the root morphology of postharvest cabbage. As shown in Fig. 2(b), the contact area between cutter and root gradually increased with the increase of cutter displacement in stage  $D_1$ , resulted in the linear growth of root-cutting force. The cambium of root was annular and its cells were relatively small and dense (shown in Fig. 2(c)). The shear area of annular cambium at peak  $P_1$  was the largest, so the root-cutting force was the greatest. In stage  $D_2$ , the shear area of annular cambium decreased to a stable state, and the shear area of the xylem relatively increased. Because the xylem cells were relatively larger and looser than cambium cells (shown in Fig. 2(d)), the root-cutting force at this stage was relatively reduced. With the cutter gradually approached peak  $P_2$ , the root-cutting force reached the peak again. The shear area at stage  $D_3$  gradually decreased with the increase of the cutter displacement. In a similar way, the root-cutting force in this stage also decreased linearly. In addition, it doesn't matter if it's flat-cutting

or sliding-cutting, the curve of root-cutting force with cutter displacement was always similar to the Fig. 2(a), only the total cutter displacement increased with the increase of sliding-cutting angle.

**Analysis of shear form on shear stress**

The variation of root diameter with shear position is described in Fig. 3. In general, the root diameter increased with the decrease of shear position. The difference of root diameter was small and the increase tended to be gentle at range of shear position from 0 mm to 12 mm. But the increase trend of root diameter was obvious when the shear position was within 12–20 mm.

The variation of shear stress with shear position is shown in Fig. 4. The results showed that at all shear positions, the shear stress was the maximum when the double-edged cutter was used for flat cutting, and the shear stress was the second when the single-edged cutter was used for flat cutting. However, when double-edged cutter and single-edged cutter were used for sliding cutting respectively, the shear stress appeared alternating in the range from 8 mm to 12 mm. The shear stress of sliding cutting with single-edged cutter was lower than that of sliding cutting with double-edged cutter within 0~8 mm of shear position.

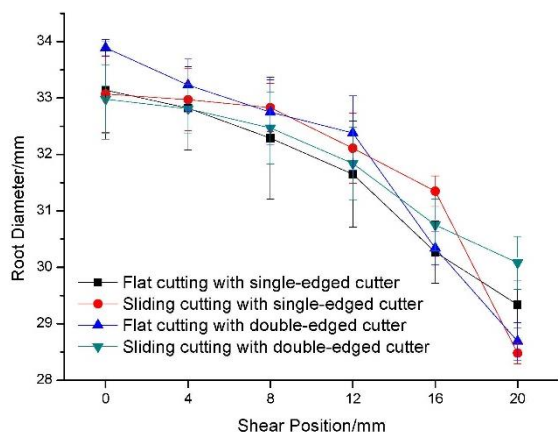


Fig. 3 - Variation of root diameter with shear position

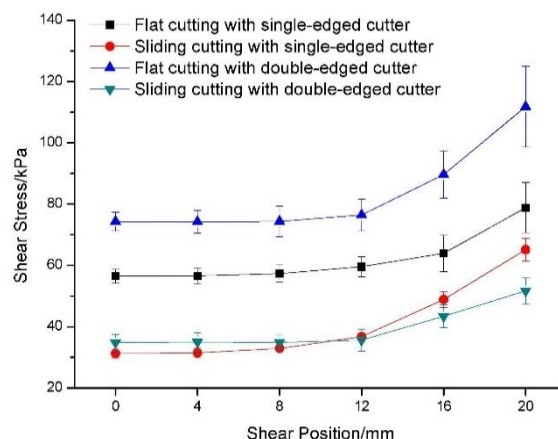


Fig. 4 - Variation of shear stress with shear position

Further analysis indicated that the shear stress gradually decreased with the decrease of shear position, regardless of the shear form. The shear position ranged from 0 mm to 12 mm was suitable for root-cutting of postharvest cabbage, the root diameter changed a little, and the shear stress tended to be stable during this range. In addition, compared with the shear stress of different shear forms, the shear stress of sliding cutting was far lower than that of flat cutting. The minimum shear stress of sliding cutting was  $31.27 \pm 1.43$  kPa when the shear position was 0 mm. Therefore, sliding cutting with single-edged cutter was selected as shear form of the orthogonal test to optimize the operation parameters of root-cutting.

**Effect of test factors on shear stress**

The results of shear orthogonal test are reported in Table 4. The shear stress of 23rd test (63.93 kPa) was the maximum and that of 13rd test (30.28 kPa) was the minimum. Regression analysis was carried out by Design Expert 10 software.

Table 4

Results of shear orthogonal test											
Number	A	B	C	D	Shear stress	Number	A	B	C	D	Shear stress
					[kPa]						[kPa]
1	-1	-1	-1	-1	44.49	16	1	1	1	1	46.54
2	1	-1	-1	-1	43.78	17	-2	0	0	0	41.41
3	-1	1	-1	-1	60.15	18	2	0	0	0	41.92
4	1	1	-1	-1	58.78	19	0	-2	0	0	32.37
5	-1	-1	1	-1	43.28	20	0	2	0	0	54.67
6	1	-1	1	-1	42.2	21	0	0	-2	0	48.05
7	-1	1	1	-1	60.46	22	0	0	2	0	46.24
8	1	1	1	-1	57.76	23	0	0	0	-2	63.93
9	-1	-1	-1	1	39.63	24	0	0	0	2	42.05

Table 4 (continuation)

Number	A	B	C	D	Shear stress [kPa]	Number	A	B	C	D	Shear stress [kPa]
10	1	-1	-1	1	40.13	25	0	0	0	0	35.86
11	-1	1	-1	1	48.13	26	0	0	0	0	33.23
12	1	1	-1	1	43.97	27	0	0	0	0	37.65
13	-1	-1	1	1	30.28	28	0	0	0	0	39.73
14	1	-1	1	1	31.64	29	0	0	0	0	38.22
15	-1	1	1	1	48.54	30	0	0	0	0	41.58

A - cutter thickness; B - shear position; C - shear speed; D - sliding-cutting angle.

The regression equation of shear stress by dimensionless coded values is shown in equation (3):

$$P_s = 37.71 - 0.38A + 6.40B - 0.92C - 5.24D - 0.64AB + 0.083AC + 0.097AD + 1.43BC - 1.12BD - 0.71CD + 0.97A^2 + 1.44B^2 + 2.34C^2 + 3.80D^2 \quad (3)$$

The regression equation of shear stress by actual values is shown in equation (4):

$$P_s = 122.42 - 46.79T_c + 0.98L_s - 0.16V_s - 2.42A_s - 1.07T_cL_s + 4.13 \times 10^{-3}T_cV_s + 0.05T_cA_s + 4.77 \times 10^{-3}L_sV_s - 0.04L_sA_s - 7.10 \times 10^{-4}V_sA_s + 24.31T_c^2 + 0.16L_s^2 + 2.34 \times 10^{-4}V_s^2 + 0.04A_s^2 \quad (4)$$

The adjusted determination coefficient ( $R^2$ ) was 0.9642, and Pred R-Squared and Adj R-Squared were 0.8735 and 0.9307 respectively, the difference between them was less than 0.2. Therefore, the factors in regression analysis could explain the test indexes well. The analysis of variance (ANOVA) of the results is shown in Table 5, the model was extremely significant ( $P < 0.0001$ ), and the lack of fit was not significant ( $P = 0.8557 > 0.1$ ). The significance order of single factor was  $B > D > C > A$ , and the significance order of interaction was  $BC > BD > CD > AB > AD > AC$ . Shear position (B), shear speed (C) and sliding-cutting angle (D) had significant effects on shear stress, while interaction between shear position and shear speed (BC) and interaction between shear position and sliding-cutting angle (BD) had significant effects on shear stress.

Table 5

ANOVA of the results

Source	Sum of squares	Freedom	Mean square	F value	P value
Model	2233.19	14	159.51	28.84	<0.0001 ***
A	3.48	1	3.48	0.63	0.4400
B	981.76	1	981.76	177.48	<0.0001 ***
C	20.13	1	20.13	3.64	0.0758 *
D	659.40	1	659.40	119.20	<0.0001 ***
AB	6.63	1	6.63	1.20	0.2909
AC	0.11	1	0.11	0.020	0.8903
AD	0.15	1	0.15	0.027	0.8705
BC	32.78	1	32.78	5.92	0.0279 **
BD	20.03	1	20.03	3.62	0.0765 *
CD	8.07	1	8.07	1.46	0.2459
A <sup>2</sup>	25.94	1	25.94	4.69	0.0469 **
B <sup>2</sup>	56.58	1	56.58	10.23	0.0060 ***
C <sup>2</sup>	150.51	1	150.51	27.21	0.0001 ***
D <sup>2</sup>	396.85	1	396.85	71.74	<0.0001 ***
Residual	82.98	15	5.53		
Lack of Fit	40.16	10	4.02	0.47	0.8557
Pure Error	42.81	5	8.56		
Total	2316.17	29			

In order to further study the effect of both *BC* and *BD* on shear stress, the response surface analysis was conducted by dimensionality reduction, as reported in Fig. 5. The effect of *BC* on shear stress is shown in Fig. 5(a), where the cutter thickness was 1 mm and the sliding-cutting angle was 30°. When the shear speed was constant, the shear stress decreased with the decrease of shear position. But the shear stress decreased firstly and then increased with the increase of shear speed while the shear position was constant. Among them, when the shear position was less than 6 mm and the shear speed was greater than 180 mm/min, the shear stress was relatively small.

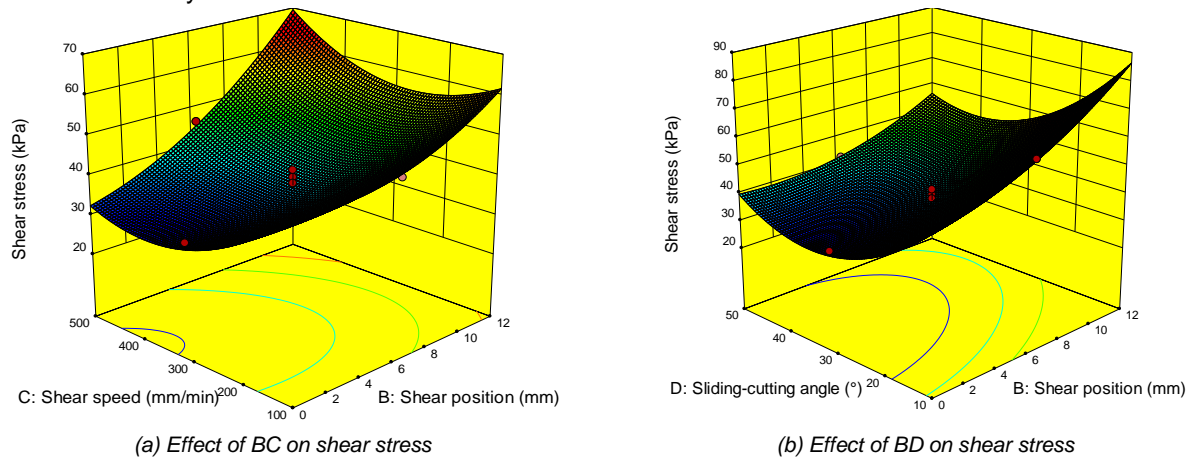


Fig. 5 - Response surface between interaction term and shear stress

Fig. 5(b) shows the effect of *BD* on shear stress, where the cutter thickness and the shear speed were 1 mm and 300 mm/min respectively. When the sliding-cutting angle was constant, the shear stress decreased with the decrease of shear position. The shear position ranged from 8 mm to 12 mm, the shear stress decreased with the increase of sliding-cutting angle. The shear position was in the range of 0–8 mm, the shear stress firstly decreased rapidly and then increased slowly with the increase of sliding-cutting angle. Among them, when the shear position was less than 4 mm and the sliding-cutting angle was greater than 18°, the shear stress was relatively small and tended to be stable.

#### Optimization of root-cutting parameters

Aiming at the minimum shear stress, the parameters were optimized by Design Expert 10 software. The results showed that when the cutter thickness was 0.89 mm, the shear position was 0.00 mm, the shear speed was 388.94 mm/min, and the sliding-cutting angle was 34.84°, the shear stress was the minimum, which was 28.02 kPa.

Based on the above optimal parameter combination, the verification test was carried out. The parameters were rounded in order to facilitate practical operation. That is, the cutter thickness was 0.9 mm, the shear position was 0.00 mm, the shear speed was 390 mm/min, and the sliding-cutting angle was 35°. On this condition, the average shear stress was 28.62±0.34 kPa, and the deviation from theoretical value of orthogonal test was 2.14%.

It could be seen from Table 4 that the results of 13rd and 14th tests were also acceptable, differed little from the shear stress on the condition of optimal parameter combination. At the same time, the shear position of 3.00 mm selected for the above tests was more practical, which could not only meet the requirements of postharvest trimming, but also avoid the damage of the head or scattering of leaf. In other words, the above combination could be selected as the parameters flexibly in the actual root-cutting operation.

## CONCLUSIONS

- 1) The curve of root-cutting force with cutter displacement was bimodal, and the peak force appeared at the maximum shear area of annular cambium, where its cells were relatively small and dense.
- 2) Shear contrast test showed that the effect of sliding-cutting with single-edged cutter was the best. The shear position ranged from 0 mm to 12 mm was suitable for root-cutting operation.
- 3) Shear orthogonal test showed that the optimal parameters of cutter thickness, shear position, shear speed and sliding-cutting angle were respectively 0.89 mm, 0.00 mm, 388.94 mm/min and 34.84°, and shear stress was 28.02 kPa. On the condition of the optimal parameters, the actual average shear stress was 28.62±0.34 kPa by verification test, and the deviation from the theoretical value was 2.14%.

**ACKNOWLEDGEMENT**

The research was supported by research grants from Shaanxi Key Research and Development Program of China (2018TSCXL-NY-05-04, 2019ZDLNY02-04), and the Scientific and Technological Achievements Promotion Program of Experiment and Demonstration Station of Northwest A&F University (TGZX2018-28).

**REFERENCES**

- [1] Cui, G. P., Zheng, X. M., Wang, J. Z., Yang, C., Liu, Z. H., & Cui, Y. J. (2019). Physical and mechanical experiments for designing cabbage precision trimming device. *The 2019 ASABE Annual International Meeting*, Boston, MA, United States. <https://doi.org/10.13031/aim.201901420>
- [2] Du, D. D., Wang, J., & Qiu, S. S. (2014). Optimization of cutting position and mode for cabbage harvesting (甘蓝根茎部切割部位及方式优化试验研究). *Transactions of the CSAE*, 30(12), 34-40. <https://doi.org/10.3969/j.issn.1002-6819.2014.12.004>
- [3] Du, D. D., Wang, J., & Qiu, S. S. (2015). Analysis and test of splitting failure in the cutting process of cabbage root. *International Journal of Agricultural and Biological Engineering*, 8(4), 27-34. <https://doi.org/10.3965/j.ijabe.20150804.1723>
- [4] Du, D. D. (2017). *Research on crawler self-propelled cabbage harvesting equipment and development of its weighing system (履带自走式甘蓝收获机研究及称重系统开发)* [Doctoral dissertation, Zhejiang University]. CNKI.
- [5] Du, D., Wang, J., Xie, L., & Deng, F. (2019). Design and field test of a new compact self-propelled cabbage harvester. *Transactions of the ASABE*, 62(5), 1243-1250. <https://doi.org/10.13031/trans.13327>
- [6] Ghahraei, O., Ahmad, D., Halina, A., Suryanto, H., & Othman, J. (2011). Cutting tests of kenaf stems. *Transactions of the ASABE*, 54(1): 51-56. <https://elibrary.asabe.org/abstract.asp?aid=36252>
- [7] Li, T. H., Meng, Z. W., Ding, H. H., Hou, J. L., Shi, G. Y., & Zhou, K. (2020). Mechanical analysis and parameter optimization of cabbage root cutting operation (甘蓝切根作业力学分析与参数优化). *Transactions of the CSAE*, 36(07): 63-72. <https://doi.org/10.11975/j.issn.1002-6819.2020.07.007>
- [8] Li, X. Q., Wang, F. E., Guo, W. J., Gong, Z. W., & Zhang, J. (2013). Influencing factor analysis of cabbage root cutting force based on orthogonal test (甘蓝根茎切割力影响因素分析). *Transactions of the CSAE*, 29(10): 42-48. <https://doi.org/10.3969/j.issn.1002-6819.2013.10.006>
- [9] Ma, Y. D., Xu, C., Cui, Y. J., Fu, L. S., Liu, H. Z., & Yang, C. (2019). Design and test of harvester for whole hydroponic lettuce with low damage (水培生菜整株低损收获装置设计与试验). *Transactions of the Chinese Society for Agricultural Machinery*, 50(01):162-169. <https://doi.org/10.6041/j.issn.1000-1298.2019.01.017>
- [10] Toncheva, N., Samsonov, A., Yegorov, V., & Lebedev, V. (2017). Results of laboratory studies of device for transporting heads to the elevator of cabbage harvest machine. *The 16th International Scientific Conference Engineering for Rural Development*, Jelgava, Latvia. <https://doi.org/10.22616/ERDev2017.16.N040>
- [11] Xu, B. S., & Yang, J. (2008). *Practical electron microscope technology (实用电镜技术)*. vol.1, Southeast University Press, Nanjing/ China, ISBN 9787564114596
- [12] Zheng, X. M., Cui, G. P., Wang, J. Z., & Cui, Y. J. (2021). Design and Experiment of Automatic Orientation Device for Post-harvest Cabbage Trimming System (甘蓝采后整修系统自动调向装置设计与试验). *Journal of Agricultural Mechanization Research*, 43(02): 64-70. <https://doi.org/10.13427/j.cnki.njyi.2021.02.011>
- [13] Zhou, C., Luan, F., Fang, X., & Chen, H. (2017). Design of cabbage pulling-out test bed and parameter optimization test. *Chemical Engineering Transactions*, 62, 1267-1272. <https://doi.org/10.3303/CET1762212>
- [14] \*\*\* MOA. (2002). *NY/T 583-2002 Cabbage (结球甘蓝)*. The Ministry of Agriculture, China. <https://kns.cnki.net/kcms/detail/detail.aspx?dbcode=SCHF&dbname=SCHF&filename=schf201909205>
- [15] \*\*\* USDA. (1997). *United States Standards for Grades of Cabbage for Processing*. United States Department of Agriculture, United States. <https://www.ams.usda.gov/grades-standards/cabbage-processing>